Green Chemistry

Accepted Manuscript

This article can be cited before page numbers have been issued, to do this please use: M. Lee, J. Hong, B. Lee, K. Ku, S. Lee, C. B. Park and K. Kang, *Green Chem.*, 2017, DOI: 10.1039/C7GC00849J.

ROYAL SOCIETY OF CHEMISTRY

rsc.li/green-chem

View Article Online
DOI: 10.1039/C7GC00849J

Green Chemistry

Paper

Multi-electron redox phenazine for ready-to-charge organic batteries

Received 00th January 20xx,
Accepted 00th January 20xx

DOI: 10.1039/x0xx00000x

www.rsc.org/

Minah Lee[a†‡], Jihyun Hong[b†], Byungju Lee[b], Kyojin Ku[b], Sechan Lee[b], Chan Beum Park[a]*, Kisuk Kang[b,c]*

Organic redox compounds represent an emerging class of cathode materials in rechargeable batteries for low-cost and sustainable energy storage. However, the low operating voltage (< 3 V) and necessity of using lithium-containing anodes have significantly limited their practical applicability to battery systems. Here, we introduce a new class of p-type organic redox centers based on N, N'-substituted phenazine (NSPZ) to build ready-to-charge organic batteries. In the absence of lithium-containing anodes, NSPZ cathodes facilitate reversible two-electron transfer at 3.7 and 3.1 V accompanying anion association, which results in a specific energy of 622 Wh kg^{-1} in dual-ion batteries.

Introduction

In designing high-performance and sustainable batteries, the major technical barriers lie in developing new electrode materials can outperform current electrode materials.[1,2] Unlike conventional transition-metal-based inorganic electrodes, organic compounds, which can be obtained from earth abundant elements with minimum carbon footprint, are highly desirable for making sustainable electrodes.[3-5] Thus, considerable efforts have been made to identify organic molecules and polymers that can reversibly react with lithium or sodium ions in rechargeable batteries. Various redox-active organic materials (e.g., conducting polymers, carbonyls, organosulfurs, and biological cofactors) have been explored thus far;[6-11] however, they still cannot rival state-of-the-art inorganic electrodes in terms of energy densities. The redox potentials rarely exceed 3 V resulting in a low-voltage cell which requires additional inactive parts in battery pack design to meet the voltage specification.[7, 12-14] More importantly, most organic compounds do not contain lithium in their natural state. Therefore, their use as cathodes in lithium-ion batteries (LIBs) must be accompanied by lithium-containing anodes (e.g., lithium metal), which raises another difficult issue.[7, 15]

Organic compounds with p-type redox activities and high redox potentials can provide new opportunities to create practically viable organic-based rechargeable LIBs. Unlike, n-type organic cathodes using alkali metal cations as charge carriers, p-type electrodes utilize molecular anions. Thus, they do not require a lithium-containing anode in LIBs, thereby presenting a significant advantage because conventional anode materials such as graphite can be used.[16, 17] Moreover, p-type cathodes are insensitive in their function to the selection of cations in the electrolyte, offering freedom in building battery systems using various types of cations (e.g., Li^+, Na^+, K^+, Mg^{2+}, and molecular ions) for the anodes.[18, 19] Although research on p-type cathodes is in its infancy, recent studies have reported a few p-type radical polymers,[17] graphite,[16, 20] and heterocyclic compounds containing sulfur or nitrogen atoms.[21-24] Even though the feasibility of p-type

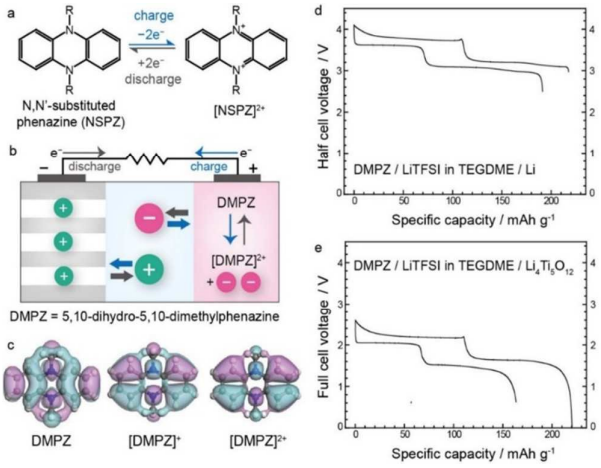

Figure 1. a) Chemical structure and redox mechanism of NSPZ. b) Schematic illustration of energy storage in dual-ion battery using DMPZ as a p-type cathode. c) HOMO plots of DMPZ and its oxidized forms. Galvanostatic charge/discharge profiles of a lithium rechargeable battery with d) DMPZ cathode and Li metal anode and e) DMPZ cathode and $Li_4Ti_5O_{12}$ anode at a current density of 50 mA g^{-1}.

[a] Department of Materials Science and Engineering, KAIST, 291 Daehak-ro, Yuseong-gu, Daejeon 34141, Republic of Korea
[b] Department of Materials Science and Engineering, Research Institute of Advanced Materials (RIAM), Seoul National University, 1 Gwanak Road, Seoul 151-742, Republic of Korea
[c] Center for Nanoparticle Research, Institute for Basic Science (IBS), Seoul National University 1 Gwanak Road, Seoul 151-742, Republic of Korea
* e-mail: matlgen1@snu.ac.kr, parkcb@kaist.ac.kr.
† These authors contributed equally.
‡ Present address: Department of Chemical Engineering, Stanford University, Stanford, CA 94305, USA
Electronic Supplementary Information (ESI) available: See DOI: 10.1039/x0xx00000x

View Article Online
DOI: 10.1039/C7GC00849J

organic cathodes was successfully demonstrated therein, these cathodes generally exhibited limited specific capacities of less than 100 mAh g^{-1}.[17, 21-23, 25] To achieve higher capacities in p-type cathodes, it is necessary to identify organic materials that are lighter and exhibit multi-electron redox capability.

To that end, here we present a new class of multi-electron p-type organic cathodes based on N, N'-substituted phenazine (NSPZ) derivatives and reveal underlying mechanisms of their redox reactions with molecular anions. The phenazines are a family of heterocyclic nitrogen-containing metabolites in living organisms, which are known to scavenge harmful radicals in biological systems and are involved with various physiological charge-transfer reactions.[26-30] We demonstrate a reversible two-electron redox reaction in NSPZ cathodes in LIBs for the first time, which exhibits an average redox potential of 3.4 V *vs.* Li/Li^+ and a theoretical capacity of 254.9 mAh g^{-1}. Combined electrochemical and structural studies reveal that anion interactions govern the reversible redox reaction of the NSPZ electrodes. We further demonstrate that the number of electrons and anions that reversibly react with the NSPZ electrode can be tuned based on the electrolyte type and salt concentration.

Experimental

Preparation of materials

5,10-Dihydro-5,10-dimethyl phenazine (DMPZ) was purchased from TCI chemicals (Japan). Other chemicals were purchased from Sigma-Aldrich (UK) and utilized without further purification. mP-DPPZ and pP-DPPZ were synthesized according to the literature.[31] A phenazine solution (1 M in o-xylene) was added to a phenyllithium solution (1.9 M in dibutyl ether) and mixed for 3h. The reaction mixture was quenched by adding cold deaerated distilled water and the organic layer was separated for following reaction. The resulting solution (2.5 mmol), which was stored with dry sodium sulfate, was further mixed with m-diiodobenzene (1 mmol), sodium tert-butoxide (3.18 mmol), bis(tri-tert-butylphosphine) palladium (0.017 mmol) at 120 °C for 1 hour. After cooling to room temperature, the mixture was filtered and the filtrate was evaporated. The residue was subjected to silica chromatography (hexane-toluene = 3:1) followed by recrystallization (tetrahydrofuran-methanol), resulting a pale yellow solid of *m*P-DPPZ. *p*P-DPPZ was prepared according to a similar procedure as for the synthesis of *m*P-DPPZ using p-diiodobenzene instead of *m*-diiodobenzene. The synthesis was performed under nitrogen atmosphere.

Electrochemistry

A three-electrode system (Pt counter electrode, $Ag/AgNO_3$ reference electrode, glassy carbon working electrode) was employed to measure solution-based cyclic voltammograms of DMPZ molecules (1 mM) at the scan rate of 100 mV s^{-1}. We used various electrolytes including $LiClO_4$, LiTFSI, $LiPF_6$, $NaClO_4$, and $MgClO_4$ in different types of solvents to test the electrolyte salt and solvent dependence of the anion-association reaction. Charge/discharge profiles of DMPZ, mp-DPPZ and pp-DPPZ powder samples were measured versus a Li metal foil (Hohsen, Japan) in coin-type cells (CR2032). The electrodes were fabricated by mixing 50% w/w active materials, 35% w/w conductive carbon (Super P) and 15% w/w polytetrafluoroehylene (PTFE) binder, which are self-standing without using any current collector. The weight of active compounds were adjusted within the range of 2.5 ± 0.5 mg per cell. A porous glassy microfiber filters (GF/F Whatman, UK) were used as separator after washed thoroughly in acetone and dried overnight at 120 °C. The composition of electrolyte salts were altered to compare the potentials of redox reaction; Electrolytes containing $LiPF_6$, (1 M), $LiClO_4$ (1 M), LiTFSI (from 0.1 M to 4.5 M) in tetraethylene glycol dimethyl ether (TEGDME) were utilized for galvanostatic measurements. The cells were assembled in an Ar-filled glove box under inert atmosphere (<0.5 ppm O_2, H_2O). Galvanostatic tests were performed at 50 mA g^{-1} current density on a battery cycler (Won-A tech, Korea).

Ex situ electrode characterization

The electrodes at different states of charge were prepared by disassembling coin cells (as-prepared, half-charged, fully charged to 4.1 V, half-discharged, and fully discharged to 2.5 V) followed by rinsing the electrodes with diethylene glycol dimethyl ether (diglyme). To prevent air contamination, all samples were prepared and sealed in an Ar-filled glove box. XPS spectra were collected with a Thermo VG Scientific Sigma Probe spectrometer (UK) equipped with a microfocus monochromated X-ray source (90 W). Binding energies were referenced to the C–C bond of the C 1s region at 284.5 eV. Fourier transform infrared spectra were obtained with pellets consisted of the mixture of electrodes and KBr powder on an FT/IR-4200 (Jasco, Japan) at a resolution of 2 cm^{-1}. Sulfur to nitrogen ratio was measured with FLASH 2000 series CHNS elemental analyzer of Thermo Scientific (UK). The results of elemental analysis were averaged after five times tests. The absorption spectrum of each sample was measured in TEGDME by a V/650 spectrophotometer (Jasco, Inc., Tokyo, Japan).

Results and discussion

Among the phenazines, NSPZ is of particular interest because of its multi-electron redox capability, as it is known to undergo two successive one-electron transfer reactions (Fig. 1a).[32] In our continuing effort to utilize a conjugated diazabutadiene motif in a heterocyclic system to store energy, for example, flavins[9, 33] and pteridines,[7] we note that NSPZ also shares the diazabutadiene motif in the heterocyclic system. Unlike flavins and pteridines, the motif in NSPZ is in its reduced form and is therefore "ready-to-charge". DMPZ, the simplest form of NSPZ, is a phenazine that is methylated at both nitrogen atoms in the pyrazine ring. Note the difference between phenazine[34] and DMPZ, which are oxidized and reduced, respectively, in pristine states. We fabricated a dual-ion rechargeable battery

View Article Online
DOI: 10.1039/C7GC00849J

system based on DMPZ as a cathode, as schematically illustrated in Fig. 1b, where the as-assembled cell was in a discharged state. The charging process leads to the oxidation of the DMPZ cathode via anion association and simultaneous reduction of the anode via cation insertion. During the discharge process, the reverse reactions occur. Therefore, the p-type DMPZ is capable of being charged even in the absence of a lithium (or sodium) reservoir in a counter electrode for lithium- (or sodium-) ion batteries.

Before the experiments, we examined the redox capability of DMPZ by calculating the highest occupied molecular orbitals (HOMO) using density functional theory (DFT) calculations to investigate the electronic stability of DMPZ during the oxidation reaction (Fig. 1c). Upon the successive removal of up to two electrons from DMPZ molecules, the electrons were effectively delocalized in the conjugated structure, implying the structural stablilty after two-electron oxidation.[35,36] Inspired by this theoretical feasibility, the electrochemical performance of DMPZ cathodes was investigated in the dual-ion batteries based on lithium ions and molecular anions [bis(trifluoromethane) sulfonamide, $TFSI^-$] at 50 mA g^{-1}, as illustrated in Fig. 1d and e. The charge–discharge profile of DMPZ in Fig. 1d reveals well-defined voltage plateaus that correspond to average potentials of 3.7 and 3.1 V (vs. Li/Li$^+$), respectively. The specific capacities were 217 and 191 mAh g^{-1} for the initial charge and discharge, respectively, which strongly indicates a two-electron redox reaction (the theoretical capacity of DMPZ for a one-electron reaction is 127.4 mAh g^{-1}). We further examined the performance of a DMPZ//$Li_4Ti_5O_{12}$-based full cell (Fig. 1e). The full cell exhibited specific capacities of 220 mAh g^{-1} (charge) and 163 mAh g^{-1} (discharge) with voltage plateaus at 2.2 and 1.6 V, respectively. This corresponds well with the result of Fig. 1d, considering the redox potential of the $Li_4Ti_5O_{12}$ electrode (~1.5 V vs. Li/Li$^+$). The reversible cycling of the full cell suggests that the dual-ion rechargeable battery system using p-type organic compounds is practically feasible.

To better understand the redox mechanism based on anion-association reaction, we investigated electrochemical activities of DMPZ by altering the electrolyte conditions. According to solution-based cyclic voltammetry (CV) analyses (Fig. 2a and Table S1), the reversibility was significantly affected by the type of electrolyte solvent. In electrolytes using low-donor-number solvents, i.e., weak Lewis bases, such as acetonitrile (ACN, 14.1)[37] and tetraglyme (TEGDME, 16.6),[38] the CV curves of DMPZ exhibited two clear pairs of redox peaks, indicative of two stable and reversible successive one-electron redox reactions. In high-donor-number solvents such as dimethyl sulfoxide (DMSO, 29.8) and dimethylformamide (DMF, 26.6), in contrast, the second cathodic peaks at 0.5 V (*vs.* Ag/$AgNO_3$, the grey dotted circle) disappeared, which suggests that the multi-electron transfer in DMPZ is no longer reversible. Instead, a new redox reaction appeared as shoulders of the first redox peaks at −0.3 to −0.2 V, which is attributed to demethylation of DMPZ during the second oxidation process in strong nucleophiles forming of 5-methylphenazinium-type products.[32] Nevertheless, when we constrained the potential window from −0.8 to 0.1 V facilitating only the first redox reaction, the redox couple was fully reversible even in DMSO and DMF (Fig. 2a, black dotted lines). These results suggest that the selection of an appropriate solvent for the electrolyte is important to fully utilize the multi-electron redox activity of the DMPZ electrode.

We further attempted to verify how the charge carriers affect the redox potential of the DMPZ electrode. As observed in Fig. 2b, we obtained identical CV curves in two different electrolytes with $LiClO_4$ and $NaClO_4$ of the same molarity, suggesting the cation selection (either Li^+ or Na^+) would not alter the electrochemical response of DMPZ in rechargeable batteries. The CV curve of DMPZ in electrolytes of a divalent cation (Mg^{2+}) with the same ClO_4^- anion reveals reversible,

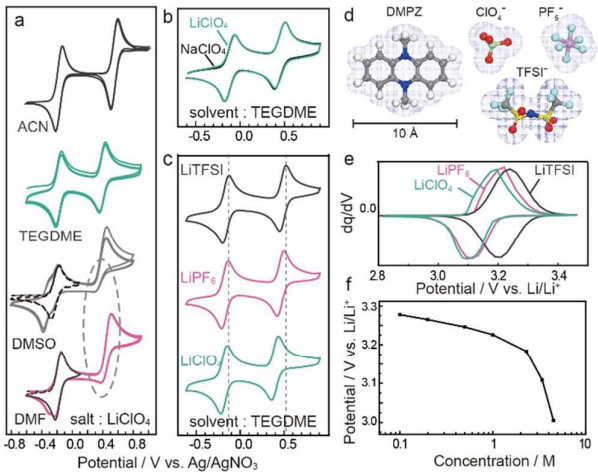

Figure 2. Combined electrochemical studies in liquid and solid states. CVs of DMPZ molecules in a) 0.1 M $LiClO_4$ in TEGDME, ACN, DMF, and DMSO, b) 0.1 M $LiClO_4$ in TEGDME and 0.1 M $NaClO_4$ in TEGDME, c) 0.1 M LiTFSI, 0.1 M $LiPF_6$, and 0.1 M $LiClO_4$ in TEGDME. d) Relative sizes of DMPZ and molecular anions including electron clouds. e) dq/dV curves of solid DMPZ electrodes in 1 M LiTFSI in TEGDME. f) Average potential of the first redox reactions measured for solid DMPZ electrodes using LiTFSI in TEGDME with various salt concentrations.

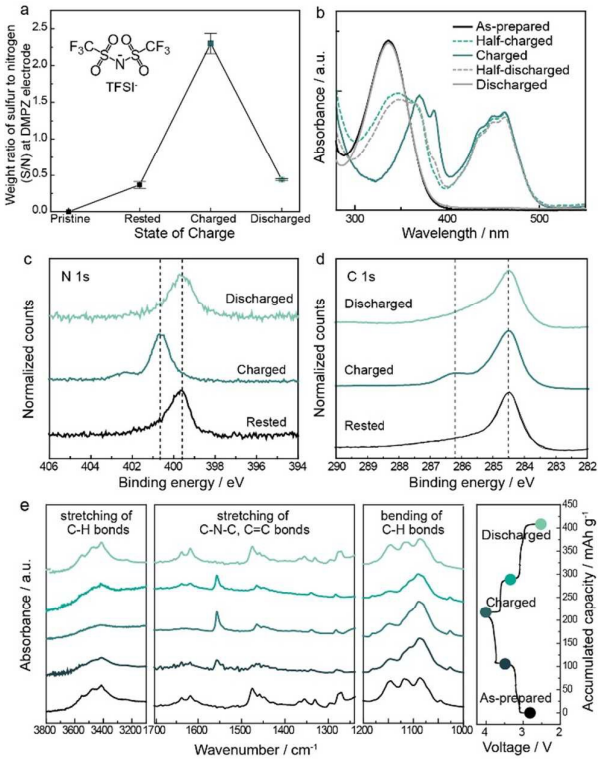

Figure 3 Ex-situ analyses of DMPZ electrodes at different states of charge in a DMPZ//Li cell. a) Sulfur to nitrogen ratio according to CHNS elemental analysis. b) UV/Vis absorption spectra. c) and d) XPS spectra of N 1s and C 1s local scan, respectively. e) FTIR spectra.

View Article Online
DOI: 10.1039/C7GC00849J

two-step redox reactions with similar potential values as those in Fig. 2b. (Fig. S1) The higher polarization might be due to the strong solvation between ions and solvent molecules. Nevertheless, this result demonstrates the possibility of utilizing DMPZ in rechargeable batteries based on multivalent cations such as Mg^{2+} and Ca^{2+}.[39]

In contrast, the redox potential of DMPZ varied notably with the type of anion species: $TFSI^-$, PF_6^-, or ClO_4^- (Fig. 2c). The redox potential of DMPZ was the highest in the electrolyte containing $TFSI^-$ ions and lowest in the one having ClO_4^- ions. We speculate that the potential change originates from the different sizes of the anions (Fig. 2d) and the resulting difference in the stability of the ($[DMPZ]^+$-$anion^-$) complexes. Large anions tend to exhibit weaker electrostatic interaction with $[DMPZ]^+$ compared with smaller anions because of the diffuse (or delocalized) nature of charge.[40] In addition, the steric effect becomes stronger as the size of anions gets bigger, which increases structural distortion and destabilizes the complex, thus resulting in a higher voltage in the electrochemical cell. This effect becomes more severe for the second redox reaction, where two anions must be associated with one molecule to compensate for the charge of $[DMPZ]^{2+}$. This description is consistent with the observation in Fig. 2c, where the variation of the second redox potential (~ 0.5 V vs. $Ag/AgNO_3$) is more significant. In coin cells using solid-state DMPZ electrodes, a similar dependence of the DMPZ redox potential on the anion type was observed (Fig. 2e), indicating the analogous electrochemical mechanism of the DMPZ in solid state.

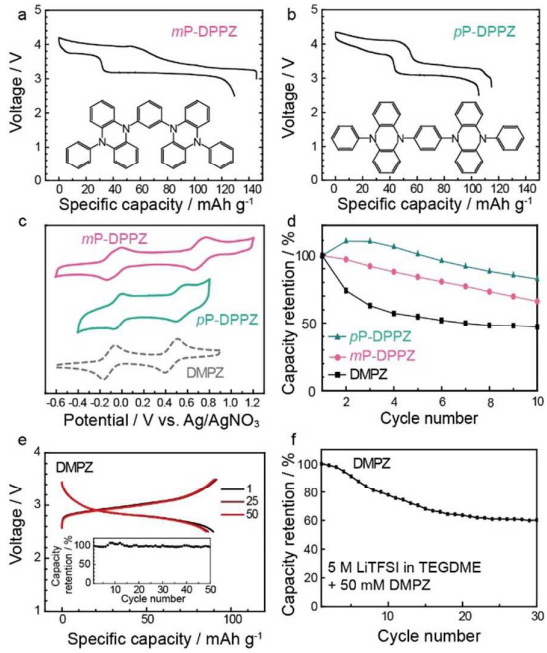

Figure 4. (a-d) Dimerization of NSPZ using phenyl groups for high performance. a) Molecular structure of two different isomeric P-DPPZs. b) CV curves of DMPZ, *m*P-DPPZ, and *p*P-DPPZ molecules in 0.1 M LiTFSI in TEGDME. c) and d) Charge/discharge profiles of P-DPPZ electrodes for five electrochemical cycles (50 mA g^{-1}). e) Voltage profile and capacity retention of DMPZ for the single-electron redox reaction. f) Capacity retention of DMPZ in 5 M electrolyte with an additive.

The anion association during battery operation is proved by the redox potential dependence on the salt concentration in electrolytes (Fig. 2f). In dilute conditions (< 1 M), the redox potential decreases linearly with the salt concentration following the Nernst equation described below (Eq. 1, 2), where the activity ($a_{[anion^-]}$) is proportional to the mole concentration. On the other hands, the redox potential should more rapidly decrease with salt concentration for high-concentration conditions (> 1 M) because the short-range ion-solvent interactions become non-negligible, resulting in a rapid increase in the activity coefficients of ions in such concentrated solution.[41-43]

$$[DMPZ] + anion^- \leftrightarrow [DMPZ]^+anion^- + e^- \qquad \text{Eq. 1}$$

$$E^{[DMPZ]/[DMPZ]+} = E^{0,[DMPZ]/[DMPZ]+} + 2.30RT/F \times \log(1/a_{[anion^-]}) \qquad \text{Eq. 2}$$

We examined the structural changes and the electron transfers in DMPZ molecules during the battery operation using *ex situ* UV/Vis absorption spectroscopy (Fig. S2b), X-ray photoelectron spectroscopy (Fig. S2c-d, and S3), and Fourier-transform infrared (FTIR) spectroscopy (Fig. S2e). We measured UV/Vis spectra of DMPZ electrodes at as-prepared, half-charged by one-electron oxidation, fully charged by two-electron oxidation, half-discharge, and fully discharged states by recollecting electrodes from coin cells disassembled at each state. The detailed analyses and discussions for the spectroscopic results are described in Supplementary Information section 2.1. The evolution of UV/Vis spectra is attributed to the step-wise transformation of neutral DMPZ into radical and divalent cations, which is fully reversible during the cycling. The reversible shift of the peaks in the N 1s and C 1s XPS spectra indicates that the diazabutadiene motif is the key redox center for the anion association reactions similar to n-type flavin[9, 33] and pteridine[36] systems. FTIR spectra verifies the reversible evolution of local bond structures in DMPZ, especially those related to C-N-C and C=C bonds, which agrees well with the XPS results. DFT calculations also support our experimental observations that the diazabutadiene motif is responsible to the reversible anion-coupled electron transfer reaction of DMPZ (Fig. S4). Overall, we confirmed that the structural evolution of DMPZ during oxidation/reduction is highly reversible and stable at molecular level.

To improve electrochemical performances of the redox active unit, we further synthesized two different dimers of NSPZ with distinct symmetry by coupling two monosubstituted 5,10-dihydrophenazine units with *m*- or *p*-diiodobenzene (Fig. 4).[31] The resulting *m*- or *p*-phenylene-linked diphenylphenazine derivatives (*m*P-DPPZ, *p*P-DPPZ) are both electrochemically active with two redox peaks in the CV curves in analogy to DMPZ (Fig. 4a-c). The dimerization strategy improved the cycle stability of the electrode due to suppressed dissolution of the molecules. This confirms that the redox motif of NSPZ can be versatilely utilized in various forms of organic compounds, providing room for designing additional NSPZ-based cathodes. We note that the limited capacity retention of the DMPZ electrode was dominantly observed for the second plateau above 3.5 V, indicating that $[DMPZ]^{2+}$ is

View Article Online
DOI: 10.1039/C7GC00849J

most soluble. As shown in Figure 4e, about 97% capacity of the initial cycle was still available in the small potential window of 2.6 to 3.5 V corresponding to the single-electron redox reaction. From the voltage profiles in various electrolyte conditions, we hypothesized that the solubility of DMPZ is insensitive to anion types (Fig. S4a), and is higher in EC/DMC than TEGDME electrolyte (Fig. S4b). Alternatively, increasing salt concentration in electrolytes improved the cycle performance of DMPZ (Fig. 4f), analogous to the solvent-in-salt approach for suppresing polysulfide dissolution in Li/Sulfur batteries.[44] With high salt concentration electrolyte containing DMPZ as a additive, the dissolution of DMPZ can be suppressed. We expect that polymerization of the redox moiety or utilization of solid electrolytes would further improve cycle life of the NSPZ-based organic cathodes. In addition, optimizing electrode architecture would improve practical applicability, for examples, encapsulating active materials in porous scaffolds for longer cycle life, and ensuring effective electronic/ionic pathways throughout the electrode for higher mass loading.[45]

Conclusions

In summary, we utilized for the first time the reduced diazabutadiene motif to facilitate anion association for energy storage by using NSPZ molecules as multi-electron-donating cathodes. Combined studies of electrochemical analyses, theoretical modeling, and ex situ spectroscopic characterization revealed the underlying mechanism for redox reactions in the p-type electrodes coupled with anion association/dissociation. The combination of salt and solvent in electrolytes strongly affects the number of electrons participating in the reversible redox reaction and alters redox potential. This study on anion-associating redox reactions presents a potential to assess high-energy, multi-electron organic electrodes for battery systems.

Acknowledgements

This study was supported by the National Research Foundation via the Creative Research Initiative Center (Grant number: NRF-2015R1A3A2066191), Republic of Korea. This work was supported by the National Research Foundation of Korea (NRF) grant funded by the Korea government (MSIP) (No. 2015R1A2A1A10055991). This work was supported by Project Code. (IBS-R006-G1).

Notes and references

1 B. Dunn, H. Kamath and J.-M. Tarascon, *Science*, 2011, **334**, 928-935.
2 D. Larcher and J.-M. Tarascon, *Nature Chemistry*, 2015, **7**, 19-29.
3 J.-M. Tarascon, *ChemSusChem*, 2008, **1**, 777-779.
4 Y. Liang, Z. Tao and J. Chen, *Advanced Energy Materials*, 2012, **2**, 742-769.
5 B. Häupler, A. Wild and U. S. Schubert, *Advanced Energy Materials*, 2015, **5**, 1402034.
6 L. Qie, L.-X. Yuan, W.-X. Zhang, W.-M. Chen and Y.-H. Huang, *Journal of The Electrochemical Society*, 2012, **159**, A1624-A1629.
7 Z. Song, Y. Qian, X. Liu, T. Zhang, Y. Zhu, H. Yu, M. Otani and H. Zhou, *Energy & Environmental Science*, 2014, **7**, 4077-4086.
8 M. Kato, K.-i. Senoo, M. Yao and Y. Misaki, *Journal of Materials Chemistry A*, 2014, **2**, 6747-6754.
9 M. Lee, J. Hong, D.-H. Seo, D. H. Nam, K. T. Nam, K. Kang and C. B. Park, *Angewandte Chemie International Edition*, 2013, **52**, 8322-8328.
10 X. Wu, S. Jin, Z. Zhang, L. Jiang, L. Mu, Y.-S. Hu, H. Li, X. Chen, M. Armand, L. Chen and X. Huang, *Science Advances*, 2015, **1**, e1500330.
11 Y. Morita, S. Nishida, T. Murata, M. Moriguchi, A. Ueda, M. Satoh, K. Arifuku, K. Sato and T. Takui, *Nature Materials*, 2011, **10**, 947-951.
12 S. Wang, L. Wang, Z. Zhu, Z. Hu, Q. Zhao and J. Chen, *Angewandte Chemie*, 2014, **126**, 6002–6006.
13 Y. Liang, P. Zhang and J. Chen, *Chemical Science*, 2013, **4**, 1330-1337.
14 T. Nokami, T. Matsuo, Y. Inatomi, N. Hojo, T. Tsukagoshi, H. Yoshizawa, A. Shimizu, H. Kuramoto, K. Komae, H. Tsuyama and J.-i. Yoshida, *Journal of the American Chemical Society*, 2012, **134**, 19694-19700.
15 D. Aurbach, E. Zinigrad, Y. Cohen and H. Teller, *Solid State Ionics*, 2002, **148**, 405-416.
16 S. Rothermel, P. Meister, G. Schmuelling, O. Fromm, H.-W. Meyer, S. Nowak, M. Winter and T. Placke, *Energ. & Environ. Sci.*, 2014, **7**, 3412-3423.
17 T. Janoschka, M. D. Hager and U. S. Schubert, *Advanced Materials*, 2012, **24**, 6397-6409.
18 X. Zhang, Y. Tang, F. Zhang and C.-S. Lee, *Advanced Energy Materials*, 2016, **6**, 1502588.
19 J. Xie, C. Li, Z. Cui and X. Guo, *Advanced Functional Materials*, 2015, **25**, 6519-6526.
20 T. Placke, S. Rothermel, O. Fromm, P. Meister, S. F. Lux, J. Huesker, H.-W. Meyer and M. Winter, *Journal of The Electrochemical Society*, 2013, **160**, A1979-A1991.
21 M. Yao, H. Sano, H. Ando and T. Kiyobayashi, *Scientific Reports*, 2015, **5**, 10962
22 M. E. Speer, M. Kolek, J. J. Jassoy, J. Heine, M. Winter, P. M. Bieker and B. Esser, *Chemical Communications*, 2015, 15261-15264.
23 W. Deng, X. Liang, X. Wu, J. Qian, Y. Cao, X. Ai, J. Feng and H. Yang, *Scientific Reports*, 2013, **3**, 2671
24 E. Deunf, P. Moreau, E. Quarez, D. Guyomard, F. Dolhem and P. Poizot, *Journal of Materials Chemistry A*, 2016, **4**, 6131-6139.
25 T. Godet-Bar, J. C. Lepretre, O. Le Bacq, J. Y. Sanchez, A. Deronzier and A. Pasturel, *Physical Chemistry Chemical Physics*, 2015, **17**, 25283-25296.
26 D. V. Mavrodi, W. Blankenfeldt and L. S. Thomashow, *Annual Review of Phytopathology*, 2006, **44**, 417-445.

View Article Online
DOI: 10.1039/C7GC00849J

27 W. S. Zaugg, *Journal of Biological Chemistry*, 1964, **239**, 3964-3970.
28 J. B. Laursen and J. Nielsen, *Chemical Reviews*, 2004, **104**, 1663-1686.
29 J.-J. Chen, W. Chen, H. He, D.-B. Li, W.-W. Li, L. Xiong and H.-Q. Yu, *Environmental Science & Technology*, 2012, **47**, 1033-1039.
30 Y. Wang and D. K. Newman, *Environmental Science & Technology*, 2008, **42**, 2380-2386.
31 E. Terada, T. Okamoto, M. Kozaki, M. E. Masaki, D. Shiomi, K. Sato, T. Takui and K. Okada, *The Journal of Organic Chemistry*, 2005, **70**, 10073-10081.
32 R. F. Nelson, D. W. Leedy, E. T. Seo and R. Adams, *Analytical and Bioanalytical Chemistry*, 1966, **224**, 184-196.
33 M. Lee, J. Hong, H. Kim, H.-D. Lim, S. B. Cho, K. Kang and C. B. Park, *Advanced Materials*, 2014, **26**, 2558-2565.
34 B. Tian, Z. Ding, G.-H. Ning, W. Tang, C. Peng, B. Liu, J. Su, C. Su and K. P. Loh, *Chemical Communications*, 2017, **53**, 2914-2917.
35 S. Wang, L. Wang, K. Zhang, Z. Zhu, Z. Tao and J. Chen, *Nano Letters*, 2013, **13**, 4404-4409.
36 J. Hong, M. Lee, B. Lee, D.-H. Seo, C. B. Park and K. Kang, *Nature Communications*, 2014, **5**, 5335.
37 B. Paduszek and M. K. Kalinowski, *Electrochimica Acta*, 1983, **28**, 639-642.
38 C. Hussey, G. Mamantov and A. Popov, *VCH, New York*, 1994, 227.
39 A. Ponrouch, C. Frontera, F. Barde and M. R. Palacin, *Nature Materials*, 2016, **15**, 169-172.
40 J. M. Pringle, J. Golding, K. Baranyai, C. M. Forsyth, G. B. Deacon, J. L. Scott and D. R. MacFarlane, *New Journal of Chemistry*, 2003, **27**, 1504-1510.
41 L. O. Valøen and J. N. Reimers, *Journal of The Electrochemical Society*, 2005, **152**, A882-A891.
42 W. W. Lucasse, *Journal of the American Chemical Society*, 1925, **47**, 743-754.
43 J. O. M. Bockris, J. O. M. Bockris and A. K. N. Reddy, *Volume 1: Modern Electrochemistry: Ionics*, Springer US, 2007.
44 L. Suo, Y.-S. Hu, H. Li, M. Armand and L. Chen, *Nature Communications*, 2013, **4**, 1481.
45 A. Vu, Y. Qian and A. Stein, *Advanced Energy Materials*, 2012, **2**, 1056-1085.